OPEN

PRS GLOBAL OPEN

ORIGINAL ARTICLE

Breast

Volume Retention, Metabolism, and Cellular Composition of Human Fat Xenografts

Brittany A. Merrifield, MD*†
Anthony Chang, PhD†‡§
Galen Hostetter, MD¶
Ewa Komorowska-Timek, MD*‖

Background: To optimize the take of transferred fat, better understanding of fat graft morphology and growth properties in vivo is critical. We aim to evaluate survival, volume retention, metabolism, and cellular composition of various aliquots of human fat xenografts.

Methods: Twenty athymic nude mice were injected subcutaneously in opposing flanks with 0.1 ml (small) and 1.0 ml (large) aliquots of human fat graft. Volume (ultrasound) of fat aliquots was measured at baseline, 1, 3, and 12 weeks after implantation. Tissue metabolism (^{18}F-FDG), Hematoxylin and Eosin, special stains, and immunohistochemical analysis were performed at 3 and 12 weeks to determine graft viability, cell origin, and proliferative activity.

Results: Only 1 of 10 small grafts were detected after 12 weeks by ultrasound and 5 of 10 were found at necropsy. Volume of large grafts decreased significantly from baseline at 3 ($827 \pm 195\,mm^3$ versus $953 \pm 122\,mm^3$; $P = 0.004$) and 12 weeks ($515 \pm 163\,mm^3$ versus $953 \pm 122\,mm^3$; $P = 0.0001$). Metabolism increased with time in small ($0.6 \pm 0.4\%$ID/g versus $2.0 \pm 1.1\%$ID/g, $P = 0.01$) and large grafts ($0.4 \pm 0.3\%$ID/g versus 1.4 ± 0.9 %ID/g; $P = 0.005$). Large grafts viability decreased between 3 and 12 weeks ($72 \pm 20\%$ versus $31 \pm 30\%$; $P = 0.012$) although small graft viability remained unchanged. Viable and proliferating human and mouse adipocytes and chimeric blood vessels were seen within grafts at both time points.

Conclusions: Larger graft aliquot was associated with better volume retention by ultrasound but lower viability by histology. Graft metabolism increased with time irrespective of aliquot size potentially due to regenerative processes of both donor and recipient origin. *(Plast Reconstr Surg Glob Open 2018;6:e1869; doi: 10.1097/GOX.0000000000001869; Published online 6 August 2018.)*

INTRODUCTION

Autologous fat transfer has been gaining popularity in breast surgery as a sole procedure or adjunctive modality to both prosthetic and autologous techniques.[1,2] Compared with more traditional reconstructive approaches, fat grafting is a less complex method with low morbidity that can be customized to address unique breast defects.[3] Despite its clinical efficacy, fat grafting is associated with some shortcomings. Fat graft take is unpredictable and ranges widely from 20% to 70%.[4] Necrotic fat can create cysts or lumps that can be oncologically concerning.[5,6] To enhance success of fat transfer, grafting using microribbons no larger than 2 mm in diameter and avoidance of larger fat aliquots associated with liponecrotic cysts has been recommended.[7] On the other hand, as demonstrated by Choi et al.[8], small fat graft volumes lead to lower volume retention than their larger counterparts.

Variable retention of transferred fat likely results from physiologic factors, which are not clearly understood. Eto et al.[9] reported 3 zones of adipocyte behavior in vitro: survival, regeneration, and necrosis depending on the fat cell distance from nutrient source. It was hypothesized that graft regeneration was dependent on a compensatory

*From the *Michigan State University College of Human Medicine, Grand Rapids, Mich.; †Small Animal Imaging Facility, Van Andel Institute, Grand Rapids, Mich.; ‡Laboratory of Translational Imaging, Van Andel Institute, Grand Rapids, Mich.; §Rethink Imaging, Grand Rapids, Mich., ¶Laboratory of Analytical Pathology, Van Andel Institute, Grand Rapids, Mich.; and ‖Advanced Plastic Surgery, Grand Rapids, Mich.*

Received for publication September 22, 2017; accepted May 23, 2018.

Supported by the Spectrum Health Research Foundation.

Ethical approval for this project was obtained by the Institutional Animal Care and Use Committee and the Spectrum Health Institutional Review Board.

DOI: 10.1097/GOX.0000000000001869

Disclosure: *The authors have no financial interest to declare in relation to the content of this article. The Article Processing Charge was paid for by the authors.*

proliferation in response to adipocyte apoptosis, in which neighboring progenitor cells become activated to maintain tissue homeostasis. In the search for the optimal fat graft aliquot, we postulate that the ultimate fat graft volume retention results from fat survival and replacement by regenerative processes of both graft and host origin. In this study, we set out to examine volume retention, metabolism, and proliferation of small and large human fat xenografts in a murine model.

METHODS

Human Lipoaspirate Harvest

Human fat was procured from a female nonsmoker undergoing a fat grafting procedure for second-stage reconstruction who consented to her own fat donation according to the Spectrum Health Institutional Review Board Protocol. The patient's thighs were injected with a standard tumescent solution composed of 1 liter of Lactated Ringer solution, 40 ml of 1% plain lidocaine, and 1 ampoule of epinephrine (1,000 units). A 5-mm fat harvesting Becker Tear Drop cannula (Byron Medical, Inc, Tucson, Ariz.) attached to standard liposuction tubing with a 60 ml Luer-lock syringe was used to manually harvest fat. The lipoaspirate was transferred to 10 ml syringes and centrifuged at 3,000 rpm for 3 minutes. After centrifugation, each syringe was placed vertically to display 3 layers: the top layer (oil), the middle layer (fat), and the bottom layer (serum). The oil and serum layers were discarded. Each syringe was then placed in a rack in vertical position, and the residual oil was removed using Codman neuropads placed on the fat layer for 4 minutes as described by Coleman.[10] The isolated human fat was then transported directly to the Van Andel Research Institute within the 10 ml syringes on ice and was immediately prepared for injection. Total time from fat harvest to injection of xenograft was 1.5 hours.

Mouse Xenograft Implantation

All animal procedures were approved by the Institutional Animal Care and Use Committee at the Van Andel Research Institute. Twenty female athymic nude mice were injected with a bolus of the human fat isolate subcutaneously with 0.1 ml (small) and 1.0 ml (large) aliquots of fat graft into right upper and left lower flank mammary fat pads, respectively. An 18 gauge needle was used to carefully place the subcutaneous injections striving for nonperitoneal penetrance. All fat xenografts were grossly visible at completion of injection. Inhalational anesthesia (2% isoflurane in 1,000 cc/min O_2) was used from initiation to completion of injections. Animals were killed at either 3 (n = 10) or 12 (n = 10) weeks after surgery.

MicroUltrasound

The animals were reanesthetized at 1, 3, and 12 weeks to undergo follow-up imaging studies. MicroUltrasound studies were performed using the Vevo 770 Imaging Platform, (Visual Sonics, Toronto, Canada). B-mode 3-D ultrasound imaging was conducted to retrieve graft and cavitations volumes immediately (baseline) and at 1, 3, and 12 weeks after grafting. Cavitations were defined as well-differentiated hypoechoic spaces within the grafts. Graft and cavitation volumes were calculated using the Visual Sonics software and reported in millimeters cubed (mm^3) and percentage of total graft volume.

Tissue Biodistribution Study

All mice were fasted with free access to water for at least 6 hours before 2′-deoxy-2′-^{18}F-fluoro-D-glucose (^{18}F-FDG) injection. The animals were placed in a 37.5 °C heated cage 20–30 minutes before radiotracer injection and moved to a 37.5 °C heated induction chamber 10 minutes before injection where they were anesthetized. A dose of 25 μCi in 0.1 ml of ^{18}F-FDG was administered through the tail vein, and the mice were placed in a 37.5°C heated induction chamber for 60 minutes of unconscious uptake. Animals were killed immediately after the uptake period at 3 and 12 weeks, and the fat grafts were collected and weighed. Radioactivity in each sample, as counts per million, was measured using the γ-scintillation counter (Perkin Elmer, Waltham, Mass.). Percentages of the injected dose/gram of tissue (%ID/g) as Standardized Metabolic Rate (SMR) were calculated for each graft by the following formula.

$$SMR = \frac{Activity_{Sample} - Activity_{Background}}{\left(Activity_{Injected} - Activity_{Background}\right)\left(Weight_{Sample}\,(g)\right)} \times 100\%$$

Fat Graft Harvest

Human fat xenografts were harvested by making an incision down the midline of the abdomen and separating the skin from the subcutaneous fascial membrane laterally to reveal the large and small grafts on either flank. Great care was taken not to disrupt the graft capsule. Grafts were harvested and placed in 10% neutral buffered formalin for 48 hours for tissue fixation, followed by embedding in paraffin block.

Histology

Hematoxylin and Eosin (H&E) staining and immunohistochemistry analysis were performed on 5 micron sections from formalin-fixed, paraffin-embedded tissues across the long axis of a graft at 3 and 12 week time points. No primary antibody slide was run as negative control. Both animal and human tissue microarrays were used in antibody optimization and contained numerous mesenchymal tissues that showed no staining. Perilipin stain was juxtaposed with respective H&E slides to assess adipocyte viability. In situ hybridization (ISH) with a human DNA-specific Alu probe was applied to visualize cells of human origin as previously described.[11] Mouse monoclonal antihuman CD34, CD24, and CD68 antibodies were utilized to identify cells of mesenchymal lineage, as follows: CD34 mesenchymal and preadipocyte, CD24 preadipocytes specific, and CD68 macrophages. Serial section immunostains and ISH assays were performed on automated immunostainer (DiscoveryUltra, Ventana, Roche Inc.). Ki-67, a cell S-phase proliferation marker, identified actively dividing cells.

Table 1. Ultrasound Volumes of Small and Large Fat Grafts at 1, 3, and 12 Weeks as Compared with Baseline

	Baseline	1 wk		3 wk		12 wk	
Graft Size	Volume (mm^3)	Volume (mm^3)	*P*	Volume (mm^3)	*P*	Volume (mm^3)	*P*
Small (n = 10)	115±51	110±50	0.09	100±40	0.09	58*	
Large (n = 10)	953±122	900±200	0.056	830±200	0.004	520±160	0.0001

*Volume of the 1 remaining graft.

In evaluating the histologic measurements, 2 investigators with mouse and human pathology research expertise reviewed adipose xenograft sections. Evaluation included the entire capsule and xenograft interface at low magnification (40×) with no less than 10 high power fields of xenograft to include both central peripheral regions.

Statistical Analysis

Ultrasound graft volume (mm^3) and cavitation data (%volume) measured at 1, 3, and 12 weeks were compared with baseline and analyzed in each animal and between the groups using paired and unpaired *t* test when appropriate. Similarly, SMR of specimens harvested at 3 and 12 weeks was compared utilizing an unpaired *t* test. The histologic measurements were evaluated statistically using paired and unpaired *t* tests when appropriate. Immune infiltrate in the capsule and within the graft was graded as 0, none; 1, minimal, few; 2, moderate; 3, moderate to marked; and 4, heavy. Organization of a capsule surrounding the grafts was measured as 0, no capsule; 1, minimal, poorly defined; 2, incomplete/cystic or delicate but well defined; 3, complete intact capsule. Presence of vasculitis was assessed as 0, none; 1, minimal; 2, moderate scattered; 3, plasma cells surrounding the vessels. All data are expressed as mean ± SD.

RESULTS

All 20 mice survived imaging studies during their respective observation periods of either 3 or 12 weeks..

MicroUltrasound

Only 1 of 10 small grafts were detected after 12 weeks by ultrasound, and 5 of 10 were found at necropsy. All large grafts were identifiable by ultrasound at 12 weeks. Small and large graft ultrasound volumes at different time points are summarized in Table 1. The volumes of the small grafts decreased from baseline by 9.4% and 12% at 1 and 3 weeks, which was not statistically significant. Only 1 small graft was detected at 12 weeks, so no average volume change could be calculated for this time point. Large graft volume significantly diminished from baseline by 13% and 46% from baseline at 3 and 12 weeks, respectively.

Table 2. SMR of Small and Large Fat Grafts at 3 and 12 Weeks (%ID/g)

Graft Size	3 wk	12 wk	*P*
Small (n = 10)	0.6±0.4	2.0±1.1*	0.01
Large (n = 10)	0.4±0.3	1.4±0.9	0.005
P	0.13	0.5	

*Only 5 small grafts were detected upon necropsy at 12 weeks.

Attempted Doppler ultrasound failed to distinguish vascularized portions of the graft due to interference of the signal form abundant skin vasculature. Large graft volume percentage cavitation did not increase from baseline at 1 week (3±1.3 %vol versus 3.3±2.3 %vol, $P = 0.76$) and at 3 weeks (3±1.3 %vol versus 5.5±4.1 %vol, $P = 0.09$), and but it increased at 12 weeks (3±1.3 %vol versus 4.5±3.0 %vol, $P < 0.05$). Cavitation could not be reliably assessed in small grafts.

Metabolic Activity

SMR of small and large grafts increased significantly from 3 to 12 weeks (Table 2). There was no difference in the SMR between small and large grafts at any time point.

Histology

Fat graft globules were well circumscribed and easily discerned from the surrounding tissues. All deposited small and large grafts were retrieved at 3 weeks; however, 10/10 large but only 5/10 small grafts were identified at 12 weeks.

H&E

Fat graft viability expressed as the percentage of viable specimen cross-section area decreased in the large and remained statistically unchanged in the small grafts over time (Fig. 1). Small and large fat graft viability was similar at 3 weeks (74±20 versus 71±20, $P = 0.87$) and at 12 weeks (55±32 versus 31±29, $P = 0.18$). Cystic formation within grafts expressed as percentage of slide section area was irrespective of aliquot size and similar at both time points (Fig. 2). H&E staining showed increased presence of ghost cells within small and large grafts with time (Table 3). Percentage of ghost cells within grafts did not differ in the small versus large specimens at 3 and 12 weeks. Similarly, the amount of immune cells within grafts remained uniform regardless of time and graft size (Table 3). Interestingly, there was no observed vasculitis within grafts at 3 weeks, whereas vasculitis was noted in small and large grafts at 12 weeks with the latter presenting a significant increase from 3 week time point (Table 3). Characteristics of capsules surrounding the grafts are depicted in Table 4. At 3 weeks, the organization of a capsule ranged from minimal to thin and well organized regardless of graft size. At 12 weeks, in contrast to small grafts, the capsules surrounding the large grafts became more defined and complete with large amounts of mouse inflammatory immune cells and greater tendency to form cysts. The small grafts that survived 12 weeks had very thin capsules that consisted largely of fibroblasts and other supportive matrix cells and less immune cells than their large counterparts. H&E staining also revealed adipocytes of various sizes, with

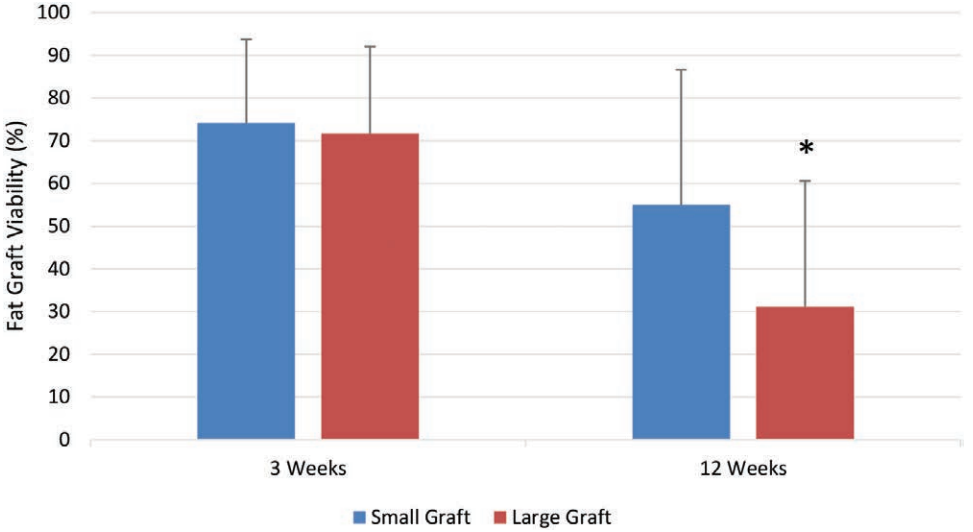

Fig. 1. Viability of small and large grafts expressed as percentage of slide cross-sectional area at 3 and 12 weeks.

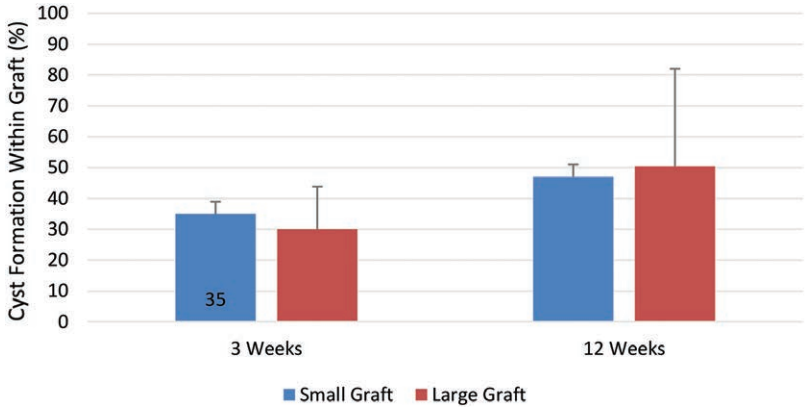

Fig. 2. Cystic formation within grafts expressed as percentage of slide cross-sectional area at 3 and 12 weeks.

Table 3. Fat Graft Characteristics

	Ghost Cells (%)		Immune Infiltrate (Grade 0–4)		Vasculitis (Grade 0–3)	
Graft Size	**3 wk**	**12 wk**	**3 wk**	**12 wk**	**3 wk**	**12 wk**
Small* (n = 10)	35±22	47±35†	2.9±1.2	1.7±1.3	0.0±0.0	0.8±1.1
Large (n = 10)	15±5.0	51±38†	1.8±1.5	2.1±1.4	0.0±0.0	1.2±1.3†
P	0.72	0.82	0.27	0.65	—	0.55

Immune infiltrate was graded as 0, none; 1, minimal, few; 2, moderate; 3, moderate to marked; and 4, heavy. Vasculitis was assessed as 0, none; 1, minimal; 2, moderate scattered; 3, plasma cells surrounding the vessels.
*Only 5 small fat grafts were analyzed at 12 weeks.
†$P < 0.05$, *t* test comparison of small or large fat graft feature change from 3 to 12 weeks.

certain morphologies suggesting an early developmental stage, which was further explored with antibody and proliferation marker staining.

Perilipin

Perilipin staining confirmed landscape of living versus nonliving adipocytes to determine overall architecture of grafts at 3 and 12 weeks and differentiated adipocytes from stromal cells. Moreover, perilipin staining revealed early adipocytes with frothy appearance suggesting regenerative processes of adipogenesis at 3 and 12 weeks (Fig. 3). These cells stained heavily with perilipin compared with surrounding cells.

ISH

ISH assay identified human-derived nuclei marked by chromogen-labeled, human-specific Alu DNA repeats and showed capsule surrounding the graft to be solely of

Table 4. Capsular Characteristics

	Capsular Organization (Grade 0–3)		Cellular Infiltrate (Grade 0–4)	
Graft Size	**3 wk**	**12 wk**	**3 wk**	**12 wk**
Small* (n = 10)	2.0±0.0	1.6±1.3	2.2±1.0	0.8±0.8†
Large (n = 10)	1.7±1.0	2.9±0.3‡	2.2±2.0	2.4±1.0
P	0.09	0.01	1.0	0.01

Capsular organization was measured as 0, no capsule; 1, minimal, poorly defined; 2, incomplete/cystic or delicate but well defined; 3, complete intact capsule. Cellular infiltrate was graded as 0, none; 1, minimal, few; 2, moderate; 3, moderate to marked; and 4, heavy.
*Only 5 small fat grafts were analyzed at 12 weeks.
†$P < 0.05$, *t* test comparison of cellular infiltrate in the small fat grafts from 3 to 12 weeks.
‡$P < 0.001$, *t* test comparison of capsular organization in the large grafts from 3 to 12 weeks.

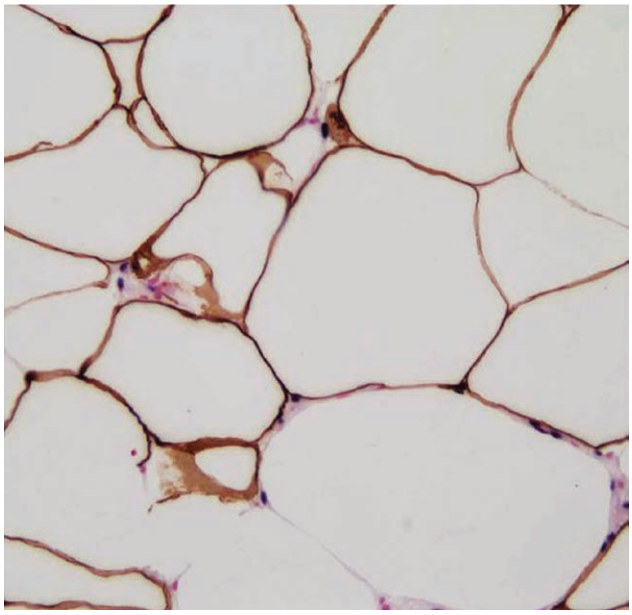

Fig. 3. Representative perilipin staining of a 12-week small graft with frothy appearance of cells indicative of early adipocytes (adipoblasts).

mouse origin. Human fat breakdown and necrosis was made evident by large amounts of human DNA present in mouse-resident macrophages located mostly in perivascular distribution in the mouse-derived capsule (Fig. 4). Additionally, ISH staining demonstrated that morphologically identified adipocytes and stromal cells within grafts (inside graft capsules) were of both human and mouse origin presenting a chimeric environment suggestive of regenerative processes (Fig. 5A, D, G). These processes were more pronounced at 12 weeks than at 3 weeks (Fig. 6).

Ki-67

Within the interior of the graft, positive nuclear staining of adipocytes with Ki-67 (S-phase proliferation marker) in sequential slices with ISH for Alu repeats indicated an active state of proliferation of human origin, particularly at 12 weeks (Fig. 5B, E, H and Fig. 6). Additionally, at both time points, capsular adipocytes stained positively with Ki-67 and lacked positive staining with ISH for human Alu repeats, pointing at regenerative contribution of the mouse, within the capsular space at the least (Fig. 6).

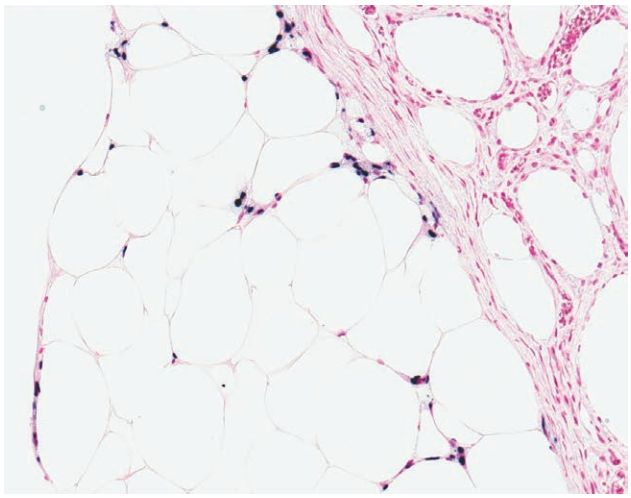

Fig. 4. ISH with human DNA Alu repeats in a 12-week large specimen. Human DNA stained in blue in mouse macrophages is located mainly in the mouse-derived graft capsule (left). This illustrates evidence of necrosis and fragmentation of human fat (lower right corner) and mouse cell activity to clear cellular debris.

CD34

To further explore regeneration and cell viability within grafts, CD 34 stain was performed. Positive CD34 may indicate presence of preadipocytes and mesenchymal cells both suggestive of active graft regeneration. Investigation of the presumed adipocyte progenitors with the CD34 did reveal smaller cells with similar morphology to adipocytes of earlier developmental stage. Staining was the strongest in comparatively smaller adipocytes with robust and discrete cell membranes and located in closer proximity to the graph periphery (Fig. 5C, F, I). Moreover, positive CD34 staining confirmed the presence of viable cells, which coincided with morphology of mature adipocytes. Negative CD34 staining was noted toward the center of the graft in cells that have lost discrete cell membranes and exhibited strong vacuole formation.

CD24

CD24 staining proved to be uninformative, due to high cross reactivity between species and cell types.

CD68

Due to the intense positive staining with Ki-67, CD68 antibody was used to rule out proliferation of macrophages, another possible cell type of mesenchymal lineage. Sequential slices revealed little to no CD68 staining in proliferating (Ki67+) human adipose xenograft cells. Splenic tissue served as a positive control and with expected distinct and localized staining.

Blood Vessel Formation

Alu-ISH–stained 12-week samples provided a method to examine the origin and formation of blood vessels within the grafts. Interestingly, blood vessels composed of both hu-

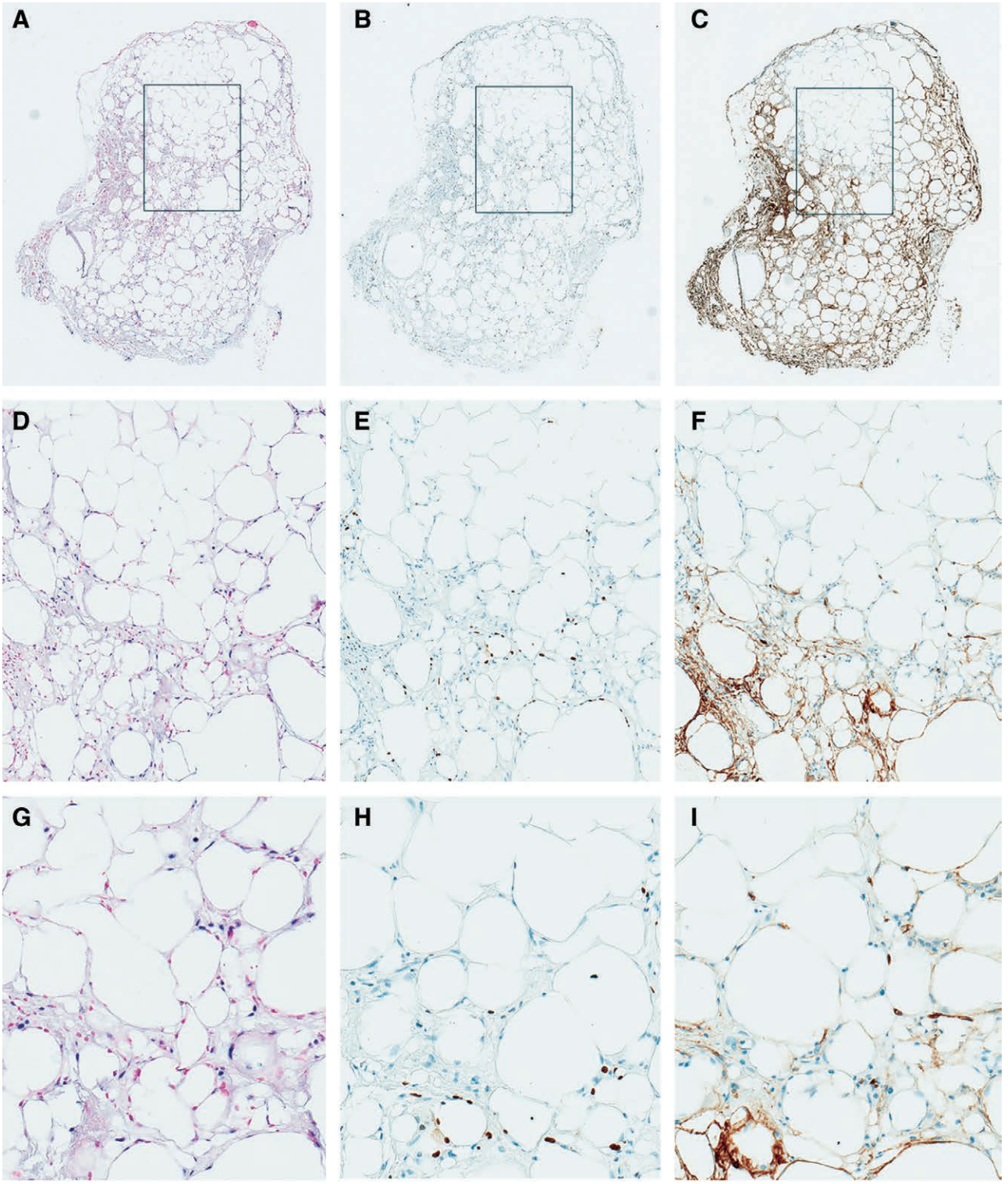

Fig. 5. Sequential cuts at 5 μm of a 12-week small graft with Alu-ISH (left column), Ki-67 (middle column), CD34 (right column) staining at 5×, 10×, and 20× magnifications displayed in respective rows from top to bottom. Note the central area of necrosis negative for all staining. Areas of viability show positive staining of human adipocyte nuclei (left column), human cell proliferation (middle column), and CD34 uptake (right column). At 20× magnification, high proliferation around single adipocyte correlates (sequential cut) well with high CD34 uptake of the same cell (arrow). Note, most proliferation is chimeric in origin and located in the center of graft.

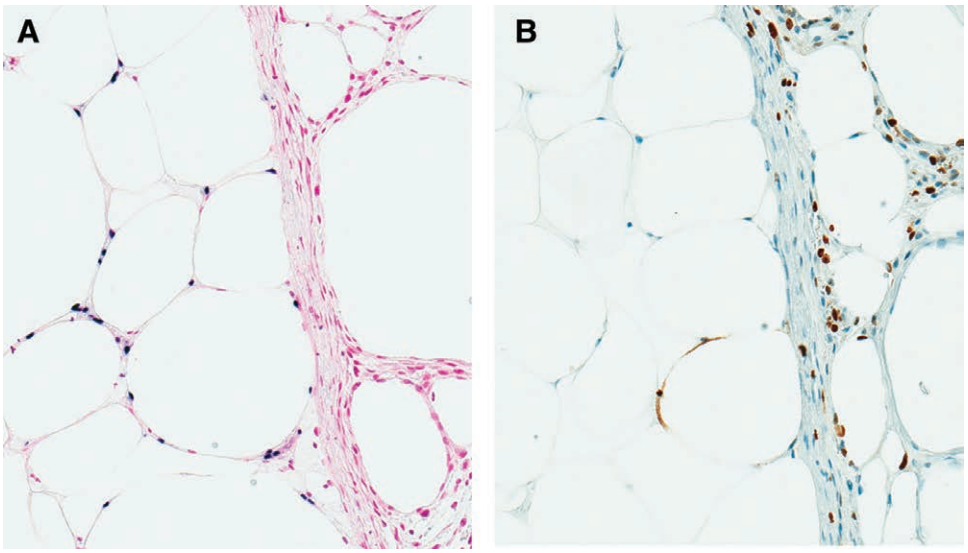

Fig. 6. A, 5 μm sequential Alu-ISH. B, Ki-67 staining of a 3-week small graft at 20× magnification. Human nuclei stained blue, mouse cells stained red, Ki-67 proliferating cells stained brown. Note evidence of mouse proliferation (red nuclei on left corresponding with brown nuclei on right) within the mouse capsule (right half). Many proliferating nucleated human cells were observed within the graft (left half). At 3 weeks, most proliferation occurred within the capsule and was of mouse origin.

man and mouse cells were noted revealing chimeric character of neovascularization. Moreover, the vessels appeared to be more chimeric in a mouse cell-predominant environment (Fig. 7), whereas, they consisted of mostly human endothelial cells in areas rich with human cells (Fig. 7).

DISCUSSION

Consistent with described clinical results,[4] variable fat graft retention was seen in our experiment. The 2 time points chosen in the study correlate clinically with early and late phases of healing: with 3 weeks marking the maximum of collagen deposition and 12 weeks reflecting more stabilized postsurgical tissue changes. Interestingly, volume of the large grafts decreased by 46% at 12 weeks, whereas only 1 of 10 small grafts could be detected by ultrasound at 12 weeks, indicating that some graft aliquots may actually be too small to survive. This observation coincides with volumetric analysis conducted by Choi et al.,

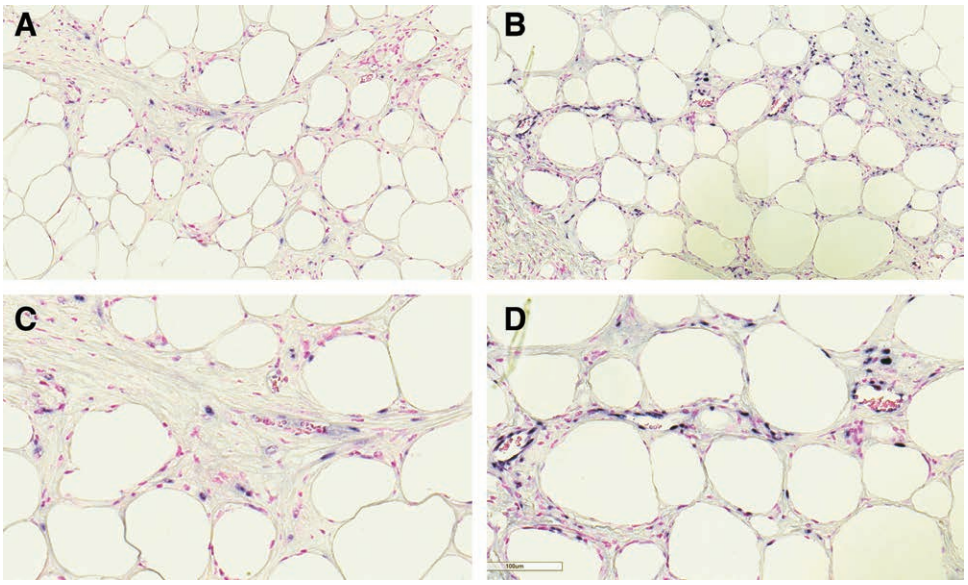

Fig. 7. The columns illustrate Alu-ISH staining in 2 separate small graft samples at 12 weeks at 10× (A, B) and 20× (C, D) demonstrating formation of chimeric and mostly human blood vessels. The left column shows chimeric vessel formation with low levels of human nuclear staining (blue) in surrounding adipocytes. The right column exhibits human vessel formation with higher background levels of human nuclear staining. More human adipocytes = more human-derived vessels.

who noted that patients with higher grafted volumes had slower volume loss and higher volume retention.[8] Clearly, fat graft deposition method employed by these authors differed from a bolus technique used in our experiment; and therefore, our observations cannot be directly extrapolated to clinical practice.

One of the shortcomings of our ultrasound evaluation was the inability to assess the volume of living fat. Cavitation corresponding to oil cyst formation was indicative of fat necrosis. Moreover, the vascularity of the remaining graft bulk could not be reliably evaluated. Histological analysis further demonstrated significant reduction of viability of large but not small grafts from 3 to 12 weeks, which was likely a reflection of progressive cell death mainly occurring in the large grafts. It is noteworthy that despite decreased graft volume, graft metabolism increased with time. We postulate this finding may be due to regenerative processes and mouse stromal ingrowth that increased demands for nutrients and cellular metabolism.

The question remains how do fat grafts survive? As suggested in the literature,[12,13] survival of fat graft may be due to persistence of the native grafted cells and/or may depend on repopulation of the original graft scaffolding by recipient cells. In our study, both proliferation of surviving donor cells and rapid cellular influx from the surrounding tissues contributed to overall graft maintenance. Although not directly investigated in our experiment, it is possible that dying cells release signals stimulating regenerative processes within the graft and adjacent tissues with the latter suggested by enhanced cellular proliferation in the mouse-derived capsules. As mentioned by Eto et al.,[9] adipocyte death can trigger fat graft regeneration cascade mediated by adipocyte-derived stems cells.

To verify the presence of cells with stem cell–like potential related to graft regeneration, we immunostained for CD34 and CD24. Adipose-derived mesenchymal stem cells have the ability to progress to an adipocyte progenitor cell and other mesenchymal cell types such as endothelial cells, macrophages, and osteoclasts.[14] The adipocyte progenitors exist in a growth-arrested state and express both CD34 and CD24.[15] Upon induction of differentiation signaling, the adipocyte progenitors will re-enter the cell cycle and begin to produce adipocyte-specific proteins.[14,15] At this stage, they are identified as cells committed to the lineage of an adipocyte, known as a committed preadipocyte. These cells continue to express CD34 but lose expression of CD24.[15] Through optimization of the CD24 antibody, we further aim to exploit this small difference between progenitor cells and committed preadipocytes in the hopes of confirming active adipose regeneration within the grafts. Figure 8 summarizes the process of adipocyte differentiation from the mesenchymal lineage that is referred to in our experiment.

To further explore regenerative processes within the graft, additional serial staining was performed. ISH for Alu repeats identified adipocyte nuclei of human origin in a chimeric environment with mouse adipocytes. Serial staining with Ki-67 (S-phase proliferation marker) identified active proliferation of human adipocytes, with higher concentrations at the graft periphery, consistent with CD34 antibody staining. Based on the positive staining with CD34 coupled with early adipocyte morphology ("frothy adipocytes"), we suspect that human origin adipose-derived mesenchymal stem cells survive grafting procedure and experience induction to adipocyte differentiation. The presence of human stromal cells in the graft indicates that the human stromal cell population either survived the grafting or was regenerated from a stem cell population. Moreover, the mouse stromal cells grew into the human fat and presumably provided scaffolding for adipocytes and initiated neovascularization. This observation is supported by the work of Planat-Benard et al.,[16] who showed the differentiation of stromal vascular fraction to endothelial cells and their incorporation into vessels promoting postischemic neovascularization in nude mice. In addition to mouse stromal cells and vasculature, human-derived vasculature was also noted. Interestingly, we observed that a higher number of human-labeled adipocytes corresponded with regions of human-origin vessels

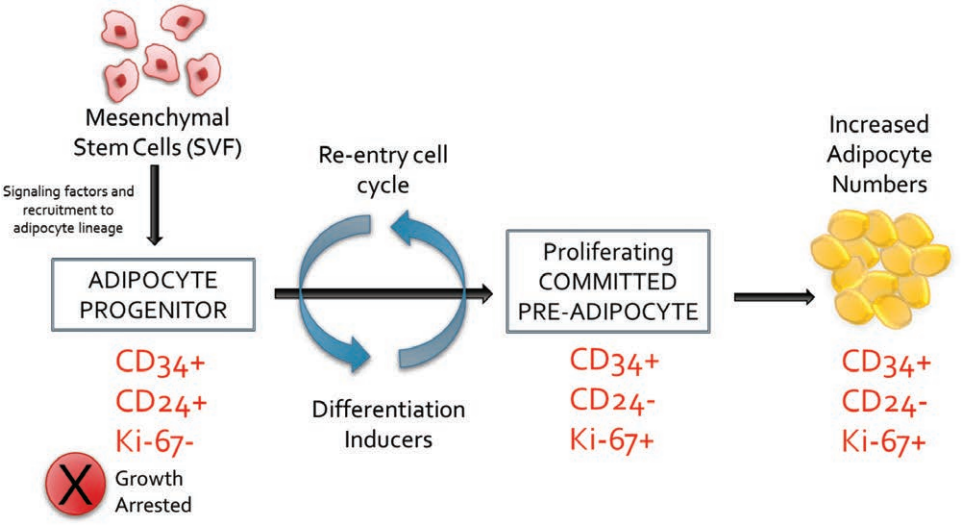

Fig. 8. Differentiation of adipocytes from mesenchymal lineage.

again emphasizing survival and growth of adipocyte and stromal donor cells. Conversely, vessels of chimeric nature were observed in mouse stroma and had a lower number of human-labeled adipocytes in adjacent regions, suggesting the important influence of mouse-derived cells in creation of chimeric fat environment.

Model Limitations

Although our human xenograft mouse model is useful for the evaluation of graft physiology and cellular proliferation, it is not a true autologous fat graft model. Therefore, the mouse antigraft immune response does not fully recapitulate graft behavior of a human autologous fat transfer. However, the unique chimeric environment characteristic of the xenograft model has elucidated the origin of proliferating cells. This adds to the knowledge of the fat physiology in vivo and confirms fat graft remodeling is influenced by both host and donor factors. Our study included only 2 time points of assessment (3 and 12 weeks), and therefore, long-term behavior of grafted fat was not investigated. Furthermore, only 2 aliquot sizes (0.1 ml and 1 ml) were used, which were an order of magnitude apart, and interspersed aliquot sizes were not grafted as is utilized clinically. However, the small graft size was selected in effort to keep with volumes of fat injected in patients. Based on the average weight of an American woman and the average total fat graft volume used clinically, the graft accounts for approximately 0.2% of total body volume. This can be compared in our model with the small graft volume accounting for 0.36% of total mouse body volume. Graft size was selected based on tolerance of the model, the predicted sensitivity of the experimental technology, and to be comparable with the human patient.

Power Limitations

The largest limitation of this study is small sample size, with just 20 mice studied and recovery of only 10% of small grafts by ultrasound. However, 100% of small grafts were detected by PET at 3 and 12 weeks and as such were included in analysis of graft metabolism. It can be noted that 5 small graft aliquots were recovered at necropsy and included in histological analysis. Although we do show confirmatory results, the lack of power in our statistical analysis presents challenge to drawing significant clinical conclusions. As we do acknowledge this important limitation, the significance of the work remains in observed overall volume loss regardless of graft size and observations made in histology work, supporting the hypothesis of graft remodeling by both host and donor factors. As the first study to examine a human fat xenograft in vivo, we believe these preliminary results support and encourage work to further confirm graft and recipient contribution to the overall survival of fat grafts. As such, the next steps for this study are to further optimize staining with CD24 antibody to differentiate stem cells committed to an adipocyte lineage and to consider fluorescence cell labeling of human fat to better characterize absorption of small grafts over time.

In conclusion, although the perfect size of fat graft aliquot was not elucidated by this study, trivial graft amounts may be inadequate to survive. Fat graft retention deteriorated with time and was accompanied by increased metabolism potentially due to regenerative processes including proliferation of graft and host adipocytes, influx of host mesenchymal cells, and formation of chimeric vessels. As survival of graft cells of mesenchymal lineage was demonstrated in our study, potential selective targeting of cellular proliferation to improve graft retention may be delivered before or after engrafting.

Ewa Komorowska-Timek, MD
Advanced Plastic Surgery
3855 Burton St SE
Grand Rapids, MI 49546
E-mail: etimek@sbcglobal.net

REFERENCES

1. de Blacam C, Momoh AO, Colakoglu S, et al. Evaluation of clinical outcomes and aesthetic results after autologous fat grafting for contour deformities of the reconstructed breast. *Plast Reconstr Surg.* 2011;128:411e–418e.
2. Sinna R, Delay E, Garson S, et al. Breast fat grafting (lipomodelling) after extended latissimus dorsi flap breast reconstruction: a preliminary report of 200 consecutive cases. *J Plast Reconstr Aesthet Surg.* 2010;63:1769–1777.
3. Brenelli F, Rietjens M, De Lorenzi F, et al. Oncological safety of autologous fat grafting after breast conservative treatment: a prospective evaluation. *Breast J.* 2014;20:159–165.
4. Dong Z, Peng Z, Chang Q, et al. The angiogenic and adipogenic modes of adipose tissue after free fat grafting. *Plast Reconstr Surg.* 2015;135:556e–567e.
5. Mizuno H, Hyakusoku H. Fat grafting to the breast and adipose-derived stem cells: recent scientific consensus and controversy. *Aesthet Surg J.* 2010;30:381–387.
6. Zimmerlin L, Donnenberg AD, Rubin JP, et al. Regenerative therapy and cancer: *in vitro* and *in vivo* studies of the interaction between adipose-derived stem cells and breast cancer cells from clinical isolates. *Tissue Eng Part A.* 2011;17:93–106.
7. Khouri RK, Rigotti G, Cardoso E, et al. Megavolume autologous fat transfer: part I. Theory and principles. *Plast Reconstr Surg.* 2014;133:550–557.
8. Choi M, Small K, Levovitz C, et al. The volumetric analysis of fat graft survival in breast reconstruction. *Plast Reconstr Surg.* 2013;131:185–191.
9. Eto H, Kato H, Suga H, et al. The fate of adipocytes after nonvascularized fat grafting: evidence of early death and replacement of adipocytes. *Plast Reconstr Surg.* 2012;129:1081–1092.
10. Coleman SR. Structural fat grafting. *Aesthet Surg J.* 1998;18:386, 388.
11. Young DM, Greulich KM, Weier HG. Species-specific in situ hybridization with fluorochrome-labeled DNA probes to study vascularization of human skin grafts on athymic mice. *J Burn Care Rehabil.* 1996;17:305–310.
12. Del Vecchio DA, Del Vecchio SJ. The graft-to-capacity ratio: volumetric planning in large-volume fat transplantation. *Plast Reconstr Surg.* 2014;133:561–569.
13. Peer LA. The neglected free fat graft, its behavior and clinical use. *Am J Surg.* 1956;92:40–47.
14. Casteilla L, Dani C. Adipose tissue-derived cells: from physiology to regenerative medicine. *Diabetes Metab.* 2006;32:393–401.
15. Jeffery E, Church CD, Holtrup B, et al. Rapid depot-specific activation of adipocyte precursor cells at the onset of obesity. *Nat Cell Biol.* 2015;17:376–385.
16. Planat-Benard V, Silvestre JS, Cousin B, et al. Plasticity of human adipose lineage cells toward endothelial cells: physiological and therapeutic perspectives. *Circulation.* 2004;109:656–663.